Lobanenkov, V. V., Plumb, M., Goodwin, G. H., & Grover, P. L. (1986) *Carcinogenesis 7*, 1689-1695.
Meehan, T., & Straub, K. (1977) *Nature 277*, 410-412.
Meehan, T., & Bond, D. M. (1984) *Proc. Natl. Acad. Sci. U.S.A. 81*, 2635-2639.
Meehan, T., Gamper, H., & Becker, J. R. (1982) *J. Biol. Chem. 257*, 10479-10485.
Osborne, M. R., Beland, F. A., Harvey, R. G., & Brookes, P. (1976) *Int. J. Cancer 18*, 362-368.
Osborne, M. R., Harvey, R. G., & Brookes, P. (1978) *Chem.-Biol. Interact. 20*, 123-130.
Osborne, M. R., Jacobs, S., Harvey, R. G., & Brookes, P. (1981) *Carcinogenesis 2*, 553-558.
Patel, D. J. (1977) *Biopolymers 16*, 2739-2754.
Patel, D. J., & Canuel, L. L. (1976) *Proc. Natl. Acad. Sci. U.S.A. 73*, 3343-3347.
Patel, D. J., & Canuel, L. L. (1977) *Proc. Natl. Acad. Sci. U.S.A. 74*, 2624-2628.
Pearl, L. H., & Neidle, S. (1986) *FEBS Lett. 209*, 269-276.
Phillips, D. H. (1983) *Nature 303*, 468-472.
Rao, S. N., Lybrand, T., Michaud, D., Jerina, D. M., & Kollman, P. A. (1989) *Carcinogenesis 10*, 27-38.
Reinhardt, C. G., & Krugh, T. R. (1978) *Biochemistry 17*, 4845-4854.
Sage, E., & Haseltine, W. A. (1984) *J. Biol. Chem. 259*, 11098-11102.
Slaga, T. J., Bracken, W. J., Gleason, G., Levin, W., Yagi, H., Jerina, D. M., & Conney, A. H. (1979) *Cancer Res. 39*, 67-71.
Sures, I., Lowry, J., & Kedes, L. H. (1978) *Cell 15*, 1033-1044.
Taylor, E. R., Miller, K. J., & Bleyer, A. J. (1983) *J. Biomol. Struct. Dyn. 1*, 883-904.
Thakker, D. R., Yagi, H., Lu, A. Y. H., Levin, W., Conney, A. H., & Jerina, D. M. (1976) *Proc. Natl. Acad. Sci. U.S.A. 73*, 3381-3385.
Thakker, D. R., Yagi, H., Akagi, H., Koreeda, M., Lu, A. Y. H., Levin, W., Wood, A. W., Conney, A. H., & Jerina, D. M. (1977) *Chem.-Biol. Interact. 16*, 281-300.
Veal, J. M., & Rill, R. L. (1988) *Biochemistry 27*, 1822-1827.
Vousden, K. H., Bos, J. L., Marshall, C. J., & Phillips, D. H. (1986) *Proc. Natl. Acad. Sci. U.S.A. 83*, 1222-1226.
Weinstein, I. B., Jeffrey, A. M., Jennette, K. W., Blobstein, S. H., Harvey, R. G., Harris, C., Autrup, H., Kasai, H., & Nakanishi, K. (1976) *Science 193*, 592-595.
Wu, R. S., Kohn, K. W., & Bonner, W. M. (1981) *J. Biol. Chem. 256*, 5916-5920.
Yang, S. K., & Gelboin, H. V. (1976) *Biochem. Pharmacol. 25*, 2221-2225.
Yang, S. K., Roller, P. P., & Gelboin, H. V. (1977) *Biochemistry 16*, 3680-3687.

# Kinetics of Interaction of Nucleotides with Nucleotide-Free H-ras p21

Jacob John, Roland Sohmen, Jürgen Feuerstein, Rosita Linke, Alfred Wittinghofer, and Roger S. Goody*
*Abteilung Biophysik, Max-Planck-Institut für medizinische Forschung, Jahnstrasse 29, 6900 Heidelberg, FRG*
*Received September 22, 1989; Revised Manuscript Received February 23, 1990*

ABSTRACT: A method is described for the convenient preparation of substantial quantities of nucleotide-free p21 or of 1:1 complexes with nucleotides other than GDP. The nucleotide-free protein has been used for kinetic studies of the binding of GDP and GTP, making use of the fluorescent analogues 3'-(methylanthraniloyl)-2'-deoxy-GDP and -GTP. Stopped-flow studies have led to the formulation of a two-step binding mechanism for both GDP and GTP, involving initial rapid but weak binding of the nucleotide followed by a relatively slow (10–20 $s^{-1}$ at 25 °C; 3–5 $s^{-1}$ at 5 °C) quasi-irreversible isomerization reaction. By use of a nonequilibrium competition method, guanosine and GMP have been shown to interact weakly but significantly with p21 (dissocation constants of 153 and 29 $\mu$M, respectively). The presence of guanosine or GMP at the active site of p21 leads to a marked stabilization of p21 against spontaneous denaturation when compared with the nucleotide- and nucleoside-free protein.

The protein product of the H-ras protooncogenes (p21)[1] is known to be a GTPase with very low GTPase activity in the isolated state [for review, see Barbacid (1987)]. The role of p21 is not known, but overexpression or mutations at certain characteristic sites lead to oncogenic transforming properties. Although earlier work indicated that transforming properties were associated with a reduction of the GTPase rate, a clear correlation of these two factors could not be demonstrated. Recently, a protein has been identified that activates the rate of GTP cleavage on the protein, leaving the rate of nucleotide (GDP) release unchanged and rate controlling in the turnover of GTP (Trahey & McCormick, 1987; Vogel et al., 1988; McCormick, 1989). This activation does not occur with transforming mutant forms of the protein. Thus, in the presence of the activating protein (GAP), whereas the cellular form of p21 exists for only a short time in the GTP bound state, transforming forms have a long-lived GTP-bound state that decays only slowly to the GDP form. According to current thinking, the GTP form of p21 is responsible for activating a process important for cell growth or differentiation, and mutants leading to a long-lived GTP-bound state result in loss of control over this process.

Since p21, like most guanine nucleotide binding proteins, binds nucleotides with an association constant of $>10^8$ $M^{-1}$, it is isolated with 1 equiv of nucleotide bound. With the protein

[1] Abbreviations: p21, protein product of the human c-Ha-ras protooncogene; GTP($\beta,\gamma$-$CH_2$), guanosine 5'-($\beta,\gamma$-methylenetriphosphate); GPPNP, guanosine 5'-($\beta,\gamma$-imidotriphosphate); mantdGDP/GTP or mdGDP/GTP, 3'-*O*-(*N*-methylanthraniloyl)-2'-deoxyguanosine di/triphosphate; EDTA, ethylenediaminetetraacetic acid; DTE, dithioerythritol.

0006-2960/90/0429-6058$02.50/0 

in this form, direct measurements of the interaction between protein and nucleotide are not possible. On the other hand, removal of the tightly bound nucleotide renders the protein thermally unstable. Thus, methods that involve long incubation times, such as equilibrium dialysis, are not applicable. Here we introduce methods that remove the tightly bound nucleotide under mild conditions and allow fluorescence measurements of the protein–nucleotide interaction. We show that both GTP and GDP binding are two-step processes, the second step presumably representing a protein isomerization. The methods are applicable to other guanine nucleotide binding proteins.

## Materials and Methods

p21 was prepared as previously described with an *Escherichia coli* expression system (Tucker at al., 1986). Tightly bound GDP was removed by the following procedure. Excess $Mg^{2+}$ was removed from the preparation (since it slows down the rate of nucleotide release; Tucker et al., 1986; Feuerstein et al., 1987b) by passage over a Sephadex PD-10 G-25 column. On a 9-mL column, 1 mL of protein solution (ca. 20 mg/mL) was applied and eluted with 4.5 mL of a $Mg^{2+}$-free, but not EDTA containing, buffer [32 mM Tris-HCl, 200 mM $(NH_4)_2SO_4$, 0.5 mM DTE, and 0.5 mM $NaN_3$ at pH 8]. The collected fraction was concentrated by centrifugation (Centricon 10 tubes, Amicon). At room temperature, the concentration of p21 was adjusted to ca. 100 $\mu$M with buffer, and GTP($\beta,\gamma$-$CH_2$) was added to a concentration that was equimolar with p21. Alkaline phosphatase (Boehringer Mannheim; ca. 2 units/mg p21) was added, and the degradation of GDP was monitored by HPLC on a RP-$C_{18}$ column under ion-pairing conditions (elution buffer was 100 mM potassium phosphate, pH 6.5, 10 mM tetrabutylammonium bromide, 0.2 mM $NaN_3$, and 3–8% acetonitrile depending on the exact characteristics of the column; isocratic elution). When all of the GDP had been converted to guanosine (typically after ca. 40 min), snake venom phosphodiesterase (ca. 20 $\mu$g/mg of p21) was added, and the degradation of GTP($\beta,\gamma$-$CH_2$) was monitored by HPLC. After this process was complete (also typically ca. 40 min), either the protein was shock frozen and stored, or guanosine was removed by gel filtration as described for the removal of $Mg^{2+}$ above.

*N*-Methylanthraniloyl derivatives of GDP, GTP, dGDP, and dGTP were prepared essentially as described by Hiratsuka (1983) for the ribonucleotides, except that a 3-fold instead of 1.5-fold excess of methylisatoic anhydride over nucleotide was used. The products were purified by ion exchange chromatography on QAE-Sephadex with a gradient of 0.2–0.5 M triethylammonium bicarbonate (pH 7.5). Purity was checked by HPLC on a RP $C_{18}$ column with a gradient of acetonitrile in 50 mM potassium phosphate (pH 6.0). The methylanthraniloyl derivatives eluted at much higher acetonitrile concentrations than the parent nucleotides.

Filter binding assays to monitor the interaction of [$^3$H]GDP with p21 were performed as previously described (Feuerstein et al., 1987a,b). Kinetic data were analyzed by nonlinear regression, normally with a single-exponential function, with the program Enzfitter (Elsevier Biosoft).

Static and slow time scale dynamic fluorescent measurements were done on an SLM 8000 spectrophotometer. For higher time resolution, a stopped-flow apparatus (Hi-Tech Scientific, Salisbury, England) was used. Excitation of the fluorescence of the methylanthraniloyl derivatives was at 366 nm, and detection was through a filter with a cutoff at 445 nm. Data were collected and analyzed with an ADS1 analog–digital converter and software package (Hi-Tech Scientific) on an Apple IIe computer. Secondary analysis was done with the program Enzfitter (Elsevier Biosoft) on a personal computer.

Scheme I

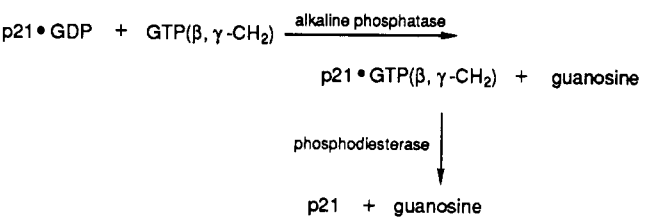


## Results and Discussion

*Removal of Bound Nucleotide from p21.* We have previously described a method for the removal of GDP from the active site of p21 (Feuerstein et al., 1987a) and were able to use the resulting nucleotide-free protein for kinetic and spectroscopic studies (Feuerstein et al., 1987b). Although this method was used extensively in studies reported by us (Feuerstein et al. 1987b; Frech et al., submitted for publication) and others (Neal et al., 1988), it was not found to be convenient for preparation of large quantities of p21 in a routine manner. This prompted us to seek a more convenient, and possibly milder, procedure than the hydrophobic interaction chromatography method used earlier. Scheme I was found to be highly reproducible and suited to preparations on a relatively large scale.

The removal and degradation of nucleotide according to Scheme I was found to be much faster than when the p21·GDP complex was simply treated with alkaline phosphatase. Since the phosphatase apparently cleaves only GDP that is free in solution (i.e., not bound to p21) and the affinity of GDP for p21 is so high, the concentration of free GDP available for degradation by the phosphatase is extremely low and many orders of magnitude below the $K_m$ value. In the presence of the phosphatase-resistant GTP analogue GTP($\beta,\gamma$-$CH_2$), although it binds approximately 100-fold more weakly than GDP (Scherer et al., 1989), the concentration of free GDP available for degradation will be greatly increased. After complete degradation of GDP, a stoichiometric complex with the analogue is obtained. This can then be relatively easily degraded by phosphodiesterase, since the rate of dissociation of the analogue is about 30-fold greater than that of GDP (data not shown). Both steps of this procedure can be monitored by reversed-phase HPLC.

For the preparation of stoichiometric complexes between p21 and GTP($\beta,\gamma$-$CH_2$) or other phosphatase-stable or -resistant analogues, the phosphodiesterase step was left out of this procedure, and alkaline phosphatase bound to agarose was used, since it can easily be removed by centrifugation after degradation of GDP. This was the method used for the preparation of the complexes between p21 and stable GTP analogues used for crystallization and X-ray structural studies (Scherer et al., 1989; Schlichting et al., 1989; Pai et al., 1989). A similar approach was used earlier for the replacement of bound guanosine nucleotides in microtubules by GTP($\beta,\gamma$-$CH_2$) (Purich & MacNeal, 1978).

The nucleotide-free p21 prepared as described above contains 2 equiv of guanosine. This can be quickly and easily removed by gel filtration, but it was found to be advantageous not to perform this step until shortly before the protein was used for experiments. This advantage stems from the observation that guanosine increases the stability of nucleotide-free p21 considerably. This is presumably caused by binding of

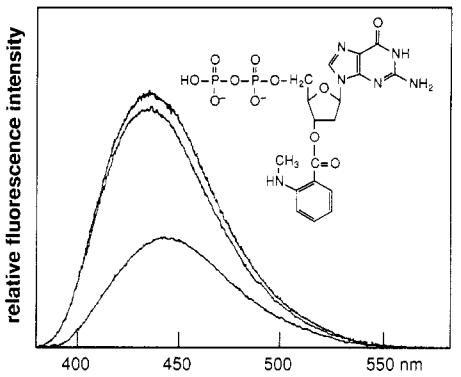


FIGURE 1: Emission spectra of (a) 2 $\mu$M 3′-(methylanthraniloyl)-2′-deoxy-GDP (structure shown in inset) in a buffer containing 64 mM Tris-HCl, pH 7.6, 1 mM EDTA, 0.5 mM DTE, and 1 mM $NaN_3$ (lower curve) and the same solution (b) after addition of 2.5 $\mu$M p21 (middle curve) and (c) after addition of 5 mM $MgCl_2$ to (b) (upper curve). Excitation wavelength 370 nm; temperature 25 °C.

guanosine to the active site, and kinetic experiments reported below confirm that this interaction does indeed occur. The half-life of nucleotide- and nucleoside-free p21 at 0 °C was found to be ca. 12 h, as measured by the loss of GDP binding ability in the filter binding assay. The stability of p21 was reduced at 25 °C, where the half-life was ca. 2 h. Addition of 1 mM guanosine led to a dramatic increase in stability, with less than 10% loss of activity occurring in 3 h at 25 °C. Stability at −70 °C was high enough to allow storage for several months. A sample stored frozen at this temperature (p21 and guanosine concentrations ca. 150 and 300 $\mu$M respectively) showed only 8% loss of GDP binding activity after 6 months.

The protein prepared by this method contains small amounts of phosphatase and phosphodiesterase and would thus not be suitable for longer incubations involving GDP or GTP.

*mantGDP as a Fluorescent Analogue of GDP.* The availability of reasonable quantities of nucleotide-free p21 allows experiments that were previously difficult or impossible to do. These include equilibrium and kinetic investigations of nucleotide binding. In order to extend the kinetic experiments into the rapid-reaction area, a spectroscopic signal is desirable as an indicator of nucleotide binding. For this reason, we prepared fluorescent derivatives of guanosine nucleotides. The derivatives chosen were the *N*-methylanthraniloyl esters of the sugar hydroxyl groups which were described by Hiratsuka (1983). Contrary to the impression given by this publication, such esters of ribonucleotides must exist as mixtures of 2′- and 3′-esters, since equilibration is known to occur under a variety of conditions. It was easily demonstrated by reversed-phase HPLC that this is indeed the case, and the two isomers were present in approximately equal quantities. These could be separated by reversed-phase HPLC but reequilibrated rapidly to the mixture. Thus we decided to prepare the methylanthraniloyl derivatives of 2′-deoxyguanosine nucleotides in order to be able to use pure substances in our experiments. We knew from independent experiments (unpublished observations) that the 2′-deoxyguanosine nucleotides bind as well as the corresponding ribonucleotides, and it was easy to show that 3′-(methylanthraniloyl)-dGDP (mantdGDP) binds strongly to p21. Using the filter binding assay described earlier, it was found that within the limits of error GDP and 3′-mantdGDP bind with equal affinity to p21 (Linke et al., unpublished results), which means that the association constant is of the order of $10^{11}$ $M^{-1}$ (Feuerstein et al., 1987).

The interaction of mantdGDP with p21 could be readily demonstrated by fluorescence spectroscopy. As shown in

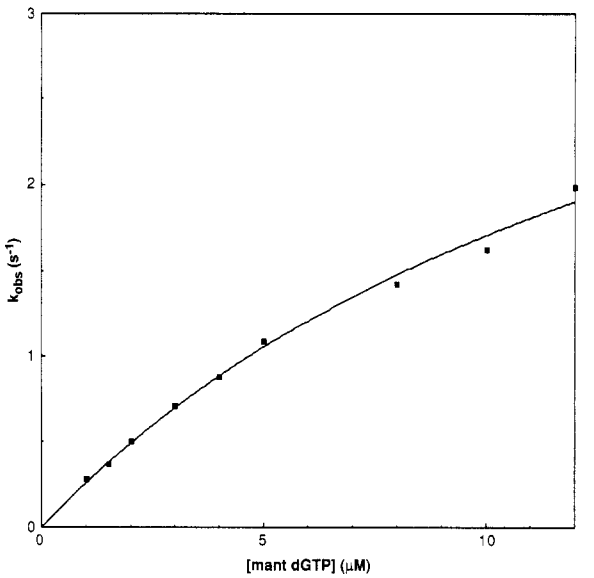


FIGURE 2: Concentration dependence of the pseudo-first-order rate constant for the association of mantdGTP with p21 at 5 °C. Conditions: 64 mM Tris-HCl, pH 7.6, 2 mM DTE, 10 mM $MgCl_2$, 1 mM $NaN_3$, and 0.5 $\mu$M p21. The solid line shows the fitted hyperbolic curve, defined by a saturating rate constant of 4.52 $s^{-1}$ and an apparent dissociation constant of 16.5 $\mu$M. It should be noted that pseudo-first-order conditions do not strictly apply to the first few points on the curve. However, the error introduced by treating the individual kinetic transients as single exponentials has been estimated to be maximally ca. 20% from simulated data for the first point and becomes negligible by the third, so that the form of the curve is not altered significantly by this effect.

Figure 1, a large increase (ca. 200% on formation of the 1:1 complex) in the intensity of the emission spectrum is seen, while the position of the maximum shifts from 441 to 432 nm (excitation wavelength 370 nm). In the absence of $Mg^{2+}$, the intensity of emission is ca. 10% lower (p21). The bound mantdGDP can be completely displaced by excess GDP (slowly in the absence of $Mg^{2+}$; very slowly in its presence), indicating that the analogue binds to the same site as GDP. Similar results were obtained with mantdGTP instead of the corresponding dGDP analogue, with no easily detectable differences in the fluorescent properties of the two enzyme–nucleotide complexes.

The change in fluorescence of mantdGDP on interacting with p21 provides a very useful signal for monitoring the binding reaction in kinetic experiments. Increasing the mantGDP concentration up to the point at which it becomes impossible to measure the rate constant due to the small amplitude of the signal in comparison with the high background from excess nucleotide leads to a linear relationship between the observed pseudo-first-order rate constant and the nucleotide concentration up to ca. 13 $\mu$M. The second-order rate constant calculated from the slope of this plot is $1.1 \times 10^6$ $M^{-1}$ $s^{-1}$ at 25 °C with excess $Mg^{2+}$, with the intercept on the *y* axis being too small to determine accurately. On cooling of the reaction to 5 °C, the corresponding rate constant dropped to $3.2 \times 10^5$ $M^{-1}$ $s^{-1}$, which is considerably smaller than that obtained earlier in our laboratory for GDP by a filter binding assay with tritium-labeled GDP ($1.7 \times 10^6$ $M^{-1}$ $s^{-1}$; Feuerstein et al., 1987b). This was surprising, since the affinity of mantGDP is similar to that of GDP and the rate constants for release of GDP and the analogue are similar, which means that the association rate constants should also be similar.

Similar experiments with mantdGTP (at 5 °C) led to the results shown in Figure 2. Here it is clear that the dependence of the pseudo-first-order rate constant does not vary in a linear

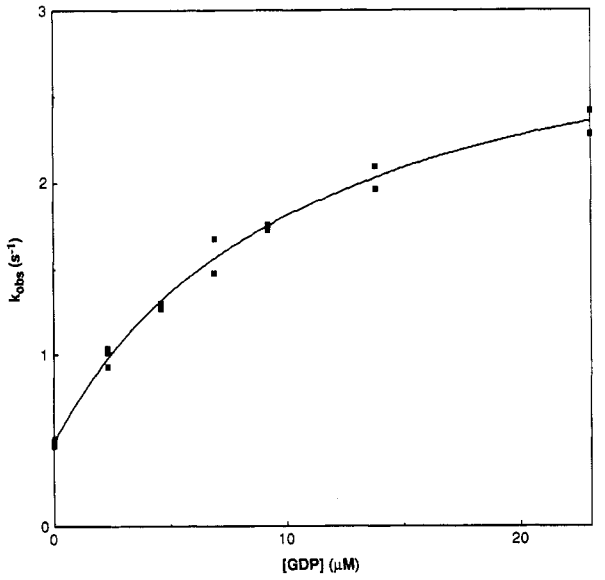


FIGURE 3: Influence of GDP concentration on the pseudo-first-order rate constant for association of 2.5 μM mantdGDP with 0.5 μM p21 at 2 °C. The error arising from analysis according to pseudo-first-order conditions in the data points at [GDP] = 0 is estimated to be ca. 5% and becomes negligible as (GDP) increases. The solid line shows the fitted curve according to eq 2 and by assuming a value of 75 μM for $1/K_{mdGDP}$. Buffer conditions were as for Figure 2.

fashion with the analogue concentration. The curvature seen does not arise from larger errors at higher concentrations of fluorophore, since the result was easily reproducible with mantdGTP, whereas mantdGDP always gave a linear plot in the same concentration range. The most obvious interpretation of these results is that binding of the nucleotide takes place in two steps. Assuming the first step to be in rapid equilibrium and the fluorescence change occurs in the second step, it can be shown that there should be a hyperbolic dependence of the rate on ligand concentration (Bagshaw et al., 1974; the equation given in this work is generally applicable for the assumed mechanism, regardless of the origin of the signal change monitored). The data shown in Figure 2 can be well fitted with a hyperbolic curve and lead to values of 16.5 μM for the dissociation constant of the first step and 4.5 $s^{-1}$ for the forward rate constant (actually the sum of the forward and reverse rate constants) for the second step at 5 °C. The linear concentration dependence of the p21–mantGDP interaction at 25 °C probably means, by analogy, that this interaction is also a two-step mechanism but that the equilibrium constant for the first step of the reaction is too small to lead to curvature of the plot under the conditions used. The question arises as to whether the observed behavior reflects a fundamental feature of the interaction between p21 and nucleotides or whether it is specific for the fluorescent GTP analogue used here. The kinetics of the interaction between GDP and GTP and p21 were thus examined, as described below.

*Interaction of GDP/GTP with p21 by Fluorescence Measurements.* Figure 3 shows the results of competition between GDP and mantdGDP during the association transient with p21. In this series of experiments, the pseudo-first-order rate constant for mantdGDP binding to p21 was measured as a function of the GDP concentration at constant mantdGDP concentration. It can be shown that for a simple (i.e., one step) binding mechanism in which the reverse rate constants are negligible, as is the case for p21 at the concentrations of nucleotides used, the following equation should describe the way in which the observed pseudo-first-order rate constant varies in this type of experiment (Fersht, 1985; Nowak & Goody, 1988):

$$k_{obs} = k_{+GDP}[GDP] + k_{+mdGDP}[mdGDP] \quad (1)$$

where $k_{+GDP}$ and $k_{+mdGDP}$ are the association rate constants for GDP and mantdGDP, respectively. In addition, the amplitude of the observed signal should decrease in a hyperbolic manner which is also a function of the concentrations and association rate constants (Nowak & Goody, 1988). According to eq 1, a plot of the observed rate constant against GDP concentration should give a straight line with slope $k_{+GDP}$ and an intercept on the $y$ axis corresponding to $k_{+mdGDP}$·[mdGDP]. The data shown in Figure 3 obviously do not follow this equation, and the most likely reason for this is that the binding mechanism is more complex than assumed, as already suggested by the results shown for mantdGTP.

There are numerous examples of two-step binding mechanisms in enzyme kinetics. A well-documented case is that of myosin ATPase, which displays a relatively weak but rapid initial binding of nucleotides followed by a quasi-irreversible isomerization step, which has been interpreted as a protein conformational change (Bagshaw et al., 1974). If a similar mechanism for p21 is assumed, the experimental situation for Figure 3 is described by the chemical equations shown in Scheme II. Here we assume that the first step is in rapid equilibrium and that the slow step in the release of GDP is $k_{-2}$, which is so small that it can be neglected. The observed rate constant for the formation of p21*·mdGDP would then be described by

$$k_{obs} = \frac{k_{+2}}{1 + (1 + K_{GDP}[GDP])/K_{mdGDP}[mdGDP]} + \frac{k'_{+2}}{1 + (1 + K_{mdGDP}[mdGDP])/K_{GDP}[GDP]} \quad (2)$$

In the experiment shown in Figure 3, the concentration of mantdGDP was such that $K_{mdGDP}(mdGDP) \ll 1$. Thus, the first term in the equation starts off being small at low [GDP] and becomes smaller in a hyperbolic fashion as [GDP] increases, finally reaching zero. The second term increases from zero to $k'_{+2}$ in a hyperbolic fashion. Thus, the observed rate constant should increase in an approximately hyperbolic fashion, as it does according to the data shown in Figure 3. The solid line in the figure shows a fit to the data according to the complete eq 2. To do this, a value of 75 μM was assumed for $1/K_{mdGDP}$, since there is insufficient information in the data to estimate $K_{mdGDP}$ and $k_{+2}$ independently. It can be seen that there is a good fit to the data, and this fit is independent of the value chosen for $1/K_{mdGDP}$ as long as this was considerably greater than the concentration of mantdGDP used in the experiment (assumption justified by data obtained at 4 °C, showing a linear relationship between the rate of binding and the concentration of mantdGDP up to at least 10 μM). The values obtained from the fit are 10.5 μM for $1/K_{GDP}$ and 3.2 $s^{-1}$ for $k'_{+2}$ at 5 °C (Table I). Thus, as for the interaction of ATP or ADP with myosin (Bagshaw et al., 1974) and for mantdGTP with p21 (Figure 2), a relatively weak interaction between p21 and GDP (or mantGDP) is followed by a highly irreversible isomerization, but in the case of p21 the rate of the isomerization in the forward direction is about an order of magnitude slower than that for myosin.

Scheme II

$$\text{p21} + \text{mdGDP} \overset{K_{mdGDP}}{\leftrightarrow} \text{p21·mdGDP} \overset{k_{+2}}{\leftrightarrow} \text{p21*·mdGDP}$$

$$\text{p21} + \text{GDP} \overset{K_{GDP}}{\leftrightarrow} \text{p21·GDP} \overset{k'_{+2}}{\leftrightarrow} \text{p21*·GDP}$$

Table I: Measured Reaction Rates and Binding Constants for p21 and Nucleotides in the Presence of 5 mM $Mg^{2+}$

| nucleotide | first step, $K_1$ ($M^{-1}$) | second step | | apparent second-order rate constant, $K_1k_{+2}$ ($M^{-1}$ $s^{-1}$) | overall affinity, $K_a$ ($M^{-1}$) |
|---|---|---|---|---|---|
| | | $k_{+2}$ ($s^{-1}$) | $k_{-2}$ ($s^{-1}$) | | |
| mantGDP (5 °C) | | | | $3.2 \times 10^5$ | $7.9 \times 10^{11}$ [a] |
| mantGDP (25 °C) | | | | $1.1 \times 10^6$ | |
| mantGTP (5 °C) | $6.1 \times 10^4$ | 4.5 | | $2.8 \times 10^5$ | $1.8 \times 10^{11}$ [a] |
| GDP (5 °C) | $9.5 \times 10^4$ | 3.2 | $5.0 \times 10^{-7}$ | $3.1 \times 10^5$ | $6.1 \times 10^{11}$ |
| GDP (25 °C) | $5.7 \times 10^4$ | 14.8 | $1.8 \times 10^{-5}$ | $8.4 \times 10^5$ | $4.6 \times 10^{10}$ |
| GTP (5 °C) | | | | $1.7 \times 10^5$ | $1.8 \times 10^{12}$ [a] |
| GTP (25 °C) | $1.25 \times 10^5$ | 16.7 | | $2.1 \times 10^6$ | |
| GMP (25 °C) | | | | | $3.5 \times 10^4$ |
| guanosine (25 °C) | | | | | $6.5 \times 10^3$ |

[a] From inhibition of GDP binding studies (Linke, 1988).

The significance and nature of the second step in the binding of nucleotides to p21 are not apparent from the present study. However, in the case of GTP, the rate constant for the second step (ca. 17 $s^{-1}$ at 25 °C; Table I) is of a magnitude similar to that of the maximally activated p21-GAP GTPase [i.e., the rate constant for GTP hydrolysis on p21 under concentration conditions that give maximal protein–protein interaction; ca. 21 $s^{-1}$ at 37 °C according to Frech et al. (submitted for publication)]. This isomerization could thus contribute to rate limitation in the complete cycle of GTP hydrolysis in vivo, which presumambly includes a catalyzed exchange of bound GDP by GTP. However, it is clear that these two steps, i.e., the isomerization identified in this work and the rate-limiting step in the experiments of Frech et al. (submitted for publication), must be different, since the starting state for the GAP-activated GTPase measurement is the preformed, and thus isomerized, p21·GTP state. In further unpublished work, we have shown that GAP does not interact with nucleotide-free p21. Thus, the isomerization may constitute the transition from a state which binds GAP weakly to a state which binds it strongly.

The apparent second-order rate constant for GDP association with p21 at concentrations much below $1/K_{GDP}$ (i.e., when the dependence of the pseudo-first-order rate constant on GDP concentration is linear) should be given by the expression $k'_{+2}/K_{GDP}$, which from the values obtained from Figure 3 would be $3.2 \times 10^5$ $M^{-1}$ $s^{-1}$. Thus, as for mantdGDP, this does not agree well with the previously published value of $1.7 \times 10^6$ $M^{-1}$ $s^{-1}$ obtained from a filter binding assay (Feuerstein et al., 1987b). For this reason, the kinetics of GDP binding to p21 were reinvestigated with the filter method in an attempt to explain the discrepancy. In order to extend the earlier work, the GDP concentration dependence of the pseudo-first-order rate constant for association with p21 was measured over a 5-fold range of GDP concentration. The results are shown in Figure 4. It can be seen that, as expected for a second-order reaction, the pseudo-first-order rate constant increases in a linear fashion. The GDP concentration used here was several orders of magnitude lower than that in the stopped-flow experiments, so that the results obtained here should correspond to the start of the curve shown in Figure 3. The slope of the curve gives an apparent second-order rate constant of $7.1 \times 10^5$ $M^{-1}$ $s^{-1}$ at 2 °C. This is considerably lower than that obtained earlier ($1.7 \times 10^6$ $M^{-1}$ $s^{-1}$; Feuerstein et al., 1987b) but is still a factor of 2 or more higher than expected from our stopped-flow work.

The reason for the discrepancy with the earlier work is apparent from Figure 4. There is a clear intercept on the $y$ axis, and since the single concentration point used for measuring and calculating the second-order rate constant in the published work was at 2.2 nM GDP, a substantial error was made by implicitly assuming that the intercept was effectively

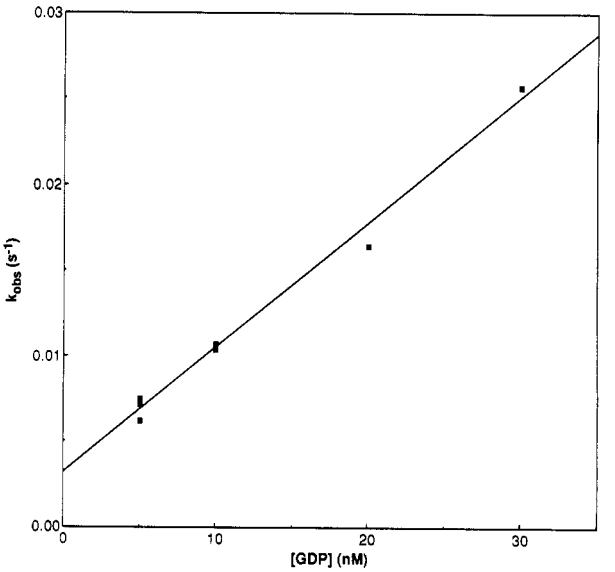


FIGURE 4: Concentration dependence of the pseudo-first-order rate constant of association of [$^3$H]GDP with 1 nM p21 from the filter binding assay at 0 °C. Buffer conditions as for Figure 2. The slope of the fitted straight line gives a value for the apparent second-order rate constant of $7.1 \times 10^5$ $M^{-1}$ $s^{-1}$.

zero. With use of the data in Figure 4, this would give a value of ca. $2 \times 10^6$ $M^{-1}$ $s^{-1}$ for this GDP concentration, which is obviously a serious overestimate of the actual rate constant but agrees well with the value calculated earlier.

The fact that a measurable intercept is seen in Figure 4 is very surprising, since this is expected to correspond to the rate constant of GDP release from its complex with p21, which we have measured to be $3 \times 10^{-5}$ $s^{-1}$ under these conditions (Feuerstein et al., 1987b). This would be too small to be detectable from the results shown in Figure 4. The finite and measurable intercept on the $y$ axis must therefore have another significance, and it is not immediately obvious what this might be. One possibility is that the binding mechanism is even more complex and that a third step occurs in the binding which is very slow, so that the initial "tightly" bound state is not the same as that formed after long incubation. Thus, the intercept in Figure 4 would correspond to the rate of dissociation from this "tight" complex, which would then be equal to $3.6 \times 10^{-3}$ $s^{-1}$, whereas on long incubation the final "very tightly" bound state would be formed. The reversal of this third step in the hypothetical binding sequence would then determine the extremely slow dissociation of the p21·GDP equilibrium complex ($5 \times 10^{-7}$ $s^{-1}$ as measured by displacement of GDP from its complex with p21 by [$^3$H]GDP).

This mechanism can be tested in the following manner. If nucleotide-free p21 is mixed with labeled GDP and at a short time after mixing a large excess of unlabeled GDP is added,

Scheme III

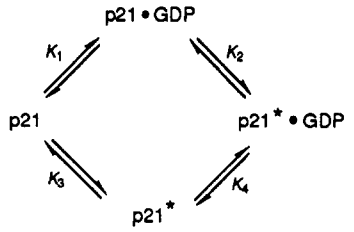


dissociation should take place from the second bound state at a rate equal to the intercept seen in Figure 3, and not at the rate of $5 \times 10^{-7}$ $s^{-1}$ seen on displacing GDP which has been allowed to equilibrate. This experiment was technically easier to perform with mantdGDP. The results showed that the rate of dissociation of the fluorescent analogue from its complex with p21 was independent of the length of time of incubation before chasing with unlabeled GDP, the reaction at ca. 2 °C being almost too slow to measure even after only 60-s incubation (data not shown). There was no trace of a faster phase corresponding to release at a rate corresponding to the $y$ axis intercept in Figure 4. A similar experiment has been performed at much lower protein and nucleotide concentrations with [$^3$H]GDP. In this case it was necessary to wait for 5 min to assure complete binding of labeled GDP before displacing with unlabeled nucleotide. Again, there was no indication of a faster phase in the dissociation. Thus, we conclude that the three-step binding mechanism as described here is not the reason for the intercept.

A plausible explanation for all the data presented on the binding kinetics is shown in Scheme III. In this scheme, the sequence of binding and isomerization reactions is assumed to be able to occur in both orders. The reaction path defined by $K_1$ and $K_2$ is equivalent to that from Scheme II, and the values chosen for the constants are those from the stopped-flow experiments ($K_1 = 10^5$ $M^{-1}$, $k_{+2} = 3.2$ $s^{-1}$, and $k_{-2} = 5 \times 10^{-7}$ $s^{-1}$). For the conversion of p21 to p21*, values of $10^{-5}$ $s^{-1}$ ($k_{+3}$) and $10^{-3}$ $s^{-1}$ ($k_{-3}$) are chosen, meaning that in the absence of nucleotide almost all of the protein would be in the p21 form. The value of $k_{-4}$ cannot be larger than that of $k_{-2}$; otherwise, GDP would dissociate via this route at the corresponding rate. We therefore choose a value that is equal to $k_{-2}$ for the sake of this argument. This fixes the value of $k_{+4}$ at $3.2 \times 10^7$ $M^{-1}$ $s^{-1}$ because of detailed balance, and this value is reasonable for a diffusion-controlled reaction. We now consider various situations with respect to nucleotide concentrations. First, at the relatively high concentrations (>1 $\mu$M) used in the stopped-flow experiments, the pseudo-first-order rate constant of association via pathway 1 (i.e., via $K_1$ and $K_2$) would be in the range of 1 $s^{-1}$ increasing hyperbolically up to a maximum of 3.2 $s^{-1}$ determined by $k_{+2}$. However, the rate constant via pathway 2 can never be faster than $k_{+3} + k_{-3}$, i.e., $10^{-3}$ $s^{-1}$. Thus, under these conditions, association would be almost entirely via pathway 1. As the concentration of GDP is reduced, the rate of association via pathway 1 will eventually be of the same order as the rate via pathway 2. With the constants chosen, the pseudo-first-order rate constant of association via pathway 2 will actually decrease with increasing nucleotide concentration, varying from $k_{+3} + k_{-3}$ at low [GDP] to $k_{+3}$ at high [GDP]. Thus, this term $k_{+3} + k_{-3}$, still remains at infinitely low nucleotide concentration, and this would correspond to the $y$ axis intercept in Figure 4. We offer this as a plausible explanation of the kinetic data presented, without placing too much significance on the exact values of the individual constants for pathway 2.

As shown in Table I the overall affinity of GDP for p21 at 5 °C is $6 \times 10^{11}$ $M^{-1}$ $s^{-1}$, confirming our earlier estimates (Feuerstein et al., 1987b) but still 2 orders of magnitude higher than the previously accepted values. A comparable affinity of $1.2 \times 10^{11}$ $M^{-1}$ has recently been reported for N-ras (Neal et al., 1988).

*Binding of Guanosine and GMP to p21.* It has long been a puzzling observation that guanine nucleotide binding proteins such as EF-Tu (Antonsson et al., 1981), transducin (Kelleher et al., 1986), and p21 (Scolnick et al., 1979) show, on the one hand, a high specificity for the guanine base and do not easily tolerate modifications (Wittinghofer et al., 1977; Linke, 1988) but, on the other hand, show an immeasurably low affinity for GMP. The reason for this could be the low sensitivity of the assays used, since the competition with the very strongly binding GDP or GTP is normally inherent to the assay principle. The availability of the kinetic methods introduced above offers a possibility of directly determining the binding constant of GMP and also of the nucleoside itself.

A different type of kinetic situation to that seen in the competitive assocation of mantdGDP/GDP or mantdGDP/GTP is expected if the association transient of mantdGDP with p21 is examined in the presence of a weakly binding ligand which is in rapid exchange with its bound form. In this case, it can be shown that, at constant mantdGDP concentration, increasing the concentration of weakly binding ligand (L) should lead to a hyperbolic decrease in the observed rate constant to a final value of zero. The exact relationship is given by

$$k_{obs} = \frac{k_{+2}}{1 + 1/K_{mdGDP}[mdGDP] + K_L[L]/K_{mdGDP}[mdGDP]} \quad (3)$$

Here $K_L$ is the effective association constant of the weak binding ligand to p21, regardless of whether this is a one- or two-step process. Under the condition that [mdGDP] $\ll 1/K_{mdGDP}$, this simplifies to $K_{mdGDP}[mdGDP]k_{+2}/(1 + K_L[L])$. Thus it should be possible to obtain binding data for very weakly binding ligands by examining their effect on the rate of mantdGDP binding to p21. The only condition is that the affinity of the ligand under investigation should be high enough for substantial binding at attainable concentrations. It does not depend on the relative binding constants of the weakly and strongly bound ligands, as in equilibrium titrations.

Although binding of guanosine to p21 could not be detected in the competitive filter binding assay, presumably due to the very large difference in the association constants of GDP and guanosine, the increased stability of the protein in the presence of 1 mM guanosine (compared to the nucleotide- and nucleoside-free form) suggested that the affinity must be high enough to allow substantial binding at this concentration. The data of Figure 5 show that this is indeed the case, since the rate of mantdGDP binding could be influenced by guanosine in the concentration range of 0–1 mM. As expected from eq 3, the observed rate constant for mantdGDP association with p21 decreases hyperbolically toward zero, with a fitted dissociation constant for guanosine ($1/K_L$) of 153 $\mu$M at 25 °C. The stabilizing effect of guanosine at 1 mM can be readily explained on the assumption that denaturation only occurs at a significant rate for the nucleotide- and nucleoside-free form of the protein, since it can be calculated with the measured dissociation constant that formation of the p21–guanosine complex occurs to the extent of ca. 85% at this concentration of free guanosine.

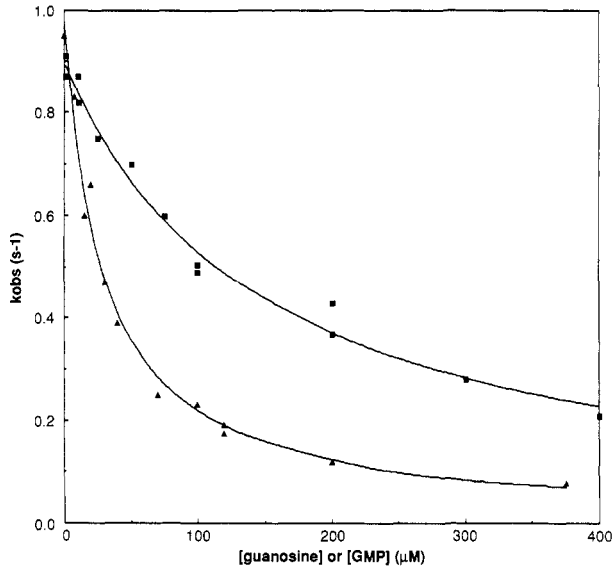


FIGURE 5: Influence of guanosine (■) and GMP (▲) on the pseudo-first-order rate constant for the interaction of 0.75 μM mantdGDP with 0.25 μM p21 at 25 °C. Buffer conditions as for Figures 2–4. The fitted hyperbolic curves give dissociation constants of 153 and 29 μM for guanosine and GMP, respectively.

Figure 5 also shows the results of a similar experiment with GMP. In this case, the dissociation constant is estimated to be 29 μM. AMP was found to have no effect at a concentration of 1 mM, as expected from the high base specificity of the nucleotide binding site. Thus, removal of the β-phosphate group of GDP leads to a reduction of affinity for p21 from ca. $10^{10}$ $M^{-1}$ to ca. $10^5$ $M^{-1}$. Since GMP interacts much more weakly with $Mg^{2+}$ than GDP, this must contribute to the low affinity for p21, since we have previously shown that $Mg^{2+}$ is coordinated to the β-phosphate of GDP (Feuerstein et al., 1987b). Even if $Mg^{2+}$ did bind to the phosphate group of GMP at the p21 active site, it would presumably be in the wrong position to interact with its protein ligands (Ser-17, Thr-35, and Asp-57 as seen from the structure of p21 with GPPNP; Pai et al., 1989). However, this can only partly explain the dramatic difference in affinities, since the reduction of affinity of GDP for p21 on removing $Mg^{2+}$ is only about a factor of 10 (Feuerstein et al., 1987b). Thus, we must conclude that there is an energetically very important interaction of the β-phosphate group with the protein. From the structure of p21 with GPPNP (Pai et al., 1989) and with GDP (DeVos et al., 1988), it can be seen that the β-phosphate of the nucleotide has many main-chain nitrogen atoms pointing toward it. In the triphosphate complex it is involved in two important interactions, one with the magnesium ion and the other with the backbone amide MH of Lys-16. It is probable that in the GDP state a third interaction with the now free third oxygen occurs, as we have previously suggested in the case of the highly homologous and structurally similar nucleotide binding domain of ribosomal elongation factor Tu (Wittinghofer et al., 1982). In contrast, as seen in the p21·GPPNP structure (Pai et al., 1989), there appears to be only one interaction of the α-phosphate group with the protein, and none with the magnesium ion, as we have shown independently using an EPR method (Feuerstein et al., 1987b). This interaction appears to be relatively weak, since it only leads to a factor of 12 preference for the "correct" diastereomer of GTP(α-S) ($S_P$ configuration) over the "wrong" diastereomer ($R_P$ configuration; Tucker et al., 1986). These arguments, together with the only moderate increase in affinity of GMP over guanosine, lead to the conclusion that there is an energetically very important interaction between the β-phosphate group and the protein (and $Mg^{2+}$) and a much weaker one to the α-phosphate. An attractive explanation for the binding behavior of GMP and GDP/GTP could be that the initial binding of all nucleotides and guanosine involves the binding site of the guanine base and that the conformational change that establishes tight binding is only possible with the β-phosphate present and involves rearrangement of the phosphate binding loop. It has been shown for adenylate kinase that the identical phosphate binding loop is very mobile and changes its structure on substrate binding (Sachsenheimer & Schulz, 1977; Dreusicke & Schulz, 1988; Reinstein et al., 1988).

It is not yet clear from the structural work on p21–nucleotide complexes or from the kinetic work described here why the affinity of GTP is not significantly higher than that of GDP. There is an additional interaction of the γ-phosphate group with $Mg^{2+}$ at the active site, but this is also present in the free (i.e., not bound to p21) Mg·GTP complex, so that it should not, to a first approximation, have a large effect, as long as the magnesium concentration is at least in the millimolar range. However, there are three further interactions of the γ-phosphate group with the protein through the backbone amides of Thr-35 and Gly-60 and the amino group of Lys-16 (Pai et al., 1989), so that there should be at least two more interactions between the protein and GTP than with GDP, perhaps more if the β,γ-bridging oxygen interacts additionally, which appears to be the case from the high-resolution structure of p21·GPPNP (Pai et al., 1990). It seems likely that the exact nature of the interactions is optimized for strong binding of GDP, which is presumably required to hold p21 in its inactive state unless GDP release is trigerred by some as yet unidentified signal.

The results reported here together with the structural analysis of the protein complexed to different nucleotides (DeVos et al., 1988; Pai et al., 1989, 1990) form the basis for further detailed analysis of the mechanism of the p21 GTPase. In the next phase of the work, it should be possible to define the mechanism at high structural resolution and at high temporal resolution, since we have been able to obtain crystals of p21 with the inert photocleavable caged GTP at the active site (Schlichting et al., 1989). After cleavage of the protecting group, hydrolysis takes place in the crystal, and the accompanying structural changes can be followed by Laue X-ray diffraction at a synchrotron source (Schlichting et al., 1990). Investigation of wild-type and mutant proteins by these combined structural and dynamic methods together with a detailed examination of the interaction of the proteins with GAP should lead to an understanding of the underlying mechanism of oncogenic transformation of p21.

Finally, it should be mentioned that the methods we have introduced here have been used by us to study the interactions between nucleotide and EF-Tu and the ralp24 protein (unpublished results). Thus they seem to be generally applicable to all guanine nucleotide binding proteins.

## ACKNOWLEDGMENTS

We thank Marija Isakov for excellent technical assistance and Ken Holmes for continued support and encouragement.

## REFERENCES

Antonsson, B., Kalbitzer, H. R., & Wittinghofer, A. (1981) *Hoppe-Seyler's Z. Physiol. Chem. 362*, 735–743.

Bagshaw, C. R., Eccleston, J. F., Eckstein, F., Goody, R. S., Gutfreund, H., & Trentham, D. R. (1974) *Biochem. J. 141*, 351–364.

Barbacid, M. (1987) *Annu. Rev. Biochem. 56*, 779–827.

DeVos, A. M., Tong, L., Milburn, M. V., Matias, P. M., Jancarik, J., Noguchi, S., Nishimura, S., Miura, K., Ohtsuka, E., & Kim, S.-H. (1988) *Science 239*, 888–893.
Dreusicke, D., & Schulz, G. E. (1988) *J. Mol. Biol. 203*, 1021–1028.
Fersht, A. (1985) *Enzyme Structure and Mechanism*, 2nd ed., p 137, W. H. Freeman, New York.
Feuerstein, J., Goody, R. S., & Wittinghofer, A. (1987a) *J. Biol. Chem. 262*, 8455–8458.
Feuerstein, J., Kalbitzer, H. R., John, J., Goody, R. S., & Wittinghofer, A. (1987b) *Eur. J. Biochem. 162*, 49–55.
Hiratsuka, T. (1983) *Biochim. Biophys. Acta 742*, 496–508.
John, J., Schlichting, I., Schiltz, E., Rösch, P., & Wittinghofer, A. (1989) *J. Biol. Chem. 264*, 13086–13092.
Kelleher, D. J., Dudycz, L. W., Wright, G. E., & Johnson, G. L. (1986) *Mol. Pharmacol. 30*, 603–608.
Linke, R. (1988) Dissertation, University of Heidelberg, FRG.
McCormick, F. (1989) *Cell 56*, 5–8.
Neal, S. E., Eccleston, J. F., Hall, A., & Webb, M. R. (1988) *J. Biol. Chem. 263*, 19718–19722.
Nowak, E., & Goody, R. S. (1988) *Biochemistry 27*, 8613–8617.
Pai, E. F., Kabsch, W., Krengel, U., Holmes, K. C., John, J., & Wittinghofer, A. (1989) *Nature 341*, 209–214.
Pai, E. F., Krengel, U., Petsko, G. A., Goody, R. S., Kabsch, W., & Wittinghofer, A. (1990) *EMBO J.* (in press).
Purich, D. L., & MacNeal, R. K. (1978) *FEBS Lett. 96*, 83–86.
Reinstein, J., Brune, M., & Wittinghofer, A. (1988) *Biochemistry 27*, 4712–4720.
Sachsenheimer, W., & Schulz, G. E. (1977) *J. Mol. Biol. 114*, 23–36.
Scherer, A., John, J., Linke, R., Goody, R. S., Wittinghofer, A., Pai, E. F., & Holmes, K. C. (1989) *J. Mol. Biol. 206*, 257–259.
Schlichting, I., Rapp, G., John, J., Wittinghofer, A., Pai, E., & Goody, R. S. (1989) *Proc. Natl. Acad. Sci. U.S.A. 86*, 7687–7690.
Schlichting, I., Almo, C., Rapp, G., Wilson, K., Petratos, K., Lentfer, A., Wittinghofer, A., Kabsch, W., Pai, E. F., Petsko, G. A., & Goody, R. S. (1990) *Nature* (in press).
Scolnick, E. M., Papageorge, A. G., & Shih, T. Y. (1979) *Proc. Natl. Acad. Sci. U.S.A. 76*, 5355–5359.
Trahey, M., & McCormick, F. (1987) *Science 238*, 542–545.
Tucker, J. Sczakiel, G., Feuerstein, J., John, J., Goody, R. S., & Wittinghofer, A. (1986) *EMBO J. 5*, 1351–1358.
Vogel, U., Dixon, R. A., Schaber, M. D., Diehl, R. E., Marshall, M. S., Scolnick, E. M., Sigal, I. S., & Gibbs, J. B. (1988) *Nature 335*, 90–93.
Wittinghofer, A., Warren, W. F., & Leberman, R. (1977) *FEBS Lett. 75*, 241–243.

# Kinetic Studies with *myo*-Inositol Monophosphatase from Bovine Brain

Axel J. Ganzhorn* and Marie-Christine Chanal
*Merrell Dow Research Institute, 16 Rue d'Ankara, F-67009 Strasbourg Cēdex, France*
*Received December 5, 1989; Revised Manuscript Received March 20, 1990*

ABSTRACT: The kinetic properties of *myo*-inositol monophosphatase with different substrates were examined with respect to inhibition by fluoride, activation or inhibition by metal ions, pH profiles, and solvent isotope effects. $F^-$ is a competitive inhibitor versus 2′-AMP and glycerol 2-phosphate, but noncompetitive ($K_{is} = K_{ii}$) versus DL-inositol 1-phosphate, all with $K_i$ values of ~45 μM. Activation by $Mg^{2+}$ follows sigmoid kinetics with Hill constants around 1.9, and random binding of substrate and metal ion. At high concentrations, $Mg^{2+}$ acts as an uncompetitive inhibitor ($K_i$ = 4.0 mM with DL-inositol 1-phosphate at pH 8.0 and 37 °C). Activation and inhibition constants, and consequently the optimal concentration of $Mg^{2+}$, vary considerably with substrate structure and pH. Uncompetitive inhibition by $Li^+$ and $Mg^{2+}$ is mutually exclusive, suggesting a common binding site. Lithium binding decreases at low pH with a p$K$ value of 6.4, and at high pH with a p$K$ of 8.9, whereas magnesium inhibition depends on deprotonation with a p$K$ of 8.3. The pH dependence of $V$ suggests that two groups with p$K$ values around 6.5 have to be deprotonated for catalysis. Solvent isotope effects on $V$ and $V/K_m$ are >2 and 1, respectively, regardless of the substrate, and proton inventories are linear. These results are consistent with a model where low concentrations of $Mg^{2+}$ activate the enzyme by stabilizing the pentacoordinate phosphate intermediate. $Li^+$ as well as $Mg^{2+}$ at inhibiting concentrations bind to an additional site in the enzyme–substrate complex. Hydrolysis of the phosphate ester is rate limiting and facilitated by acid–base catalysis.

A variety of calcium-mobilizing signals, transmitted across the cell membrane, involve the breakdown of phosphatidylinositol 4,5-bisphosphate to yield the second messengers inositol 1,4,5-trisphosphate and diacylglycerol (Berridge & Irvine, 1989; Michell et al., 1989). Brain cells lack an efficient uptake system for inositol (Spectro & Lorenzo, 1975), and resynthesis of inositol phospholipids, therefore, depends on the dephosphorylation of inositol phosphates. At least two different pathways and a number of phosphatases and kinases have been identified in the metabolism of these compounds (Majerus et al., 1988; Shears, 1989). A single enzyme, *myo*-inositol monophosphatase, hydrolyzes both enantiomers of Ins(1)P[1] and Ins(4)P (Gee et al., 1988). This is a crucial step in the mechanism of recycling, since all the pathways within the inositol lipid cycle, as well as the de novo synthesis of L-Ins(1)P from glucose 6-phosphate (Eisenberg, 1967; Mauck et al., 1980), converge at this point to replenish the pool of free inositol.

[1] Abbreviation: Ins(1)P, *myo*-inositol 1-phosphate.

0006-2960/90/0429-6065$02.50/0 